CNN CLONING TEMPLATE:
SHADOW DETECTOR

by

T. Matsumoto, L. O. Chua, and H. Suzuki

Memorandum No. UCB/ERL M90/14

28 February 1990

CNN CLONING TEMPLATE:
SHADOW DETECTOR

by

T. Matsumoto, L. O. Chua, and H. Suzuki

Memorandum No. UCB/ERL M90/14

28 February 1990

ELECTRONICS RESEARCH LABORATORY

College of Engineering
University of California, Berkeley
94720

TITLE PAGE

†This work is supported in part by the Japanese Ministry of Education, the Ogasawara Foundation, the Casio Foundation, the Institute of Science and Engineering, Waseda University and by the US office of Naval Research under grant N00014-89-J-1402 and the National Science Foundation under grant MIP86-14000.
††T.Matsumoto and H.Suzuki are with the Department of Electrical Engineering, Waseda University, Tokyo 160, Japan.
L.O.Chua is with the Department of Electrical Engineering and Computer Science, University of California, Berkeley, CA 94720

CNN CLONING TEMPLATE:
SHADOW DETECTOR

by

T. Matsumoto, L. O. Chua, and H. Suzuki

Memorandum No. UCB/ERL M90/14

28 February 1990

ELECTRONICS RESEARCH LABORATORY

College of Engineering
University of California, Berkeley
94720

[†]This work is supported in part by the Japanese Ministry of Education, the Ogasawara Foundation, the Casio Foundation, the Institute of Science and Engineering, Waseda University and by the US office of Naval Research under grant N00014-89-J-1402 and the National Science Foundation under grant MIP86-14000.

[††]T.Matsumoto and H.Suzuki are with the Department of Electrical Engineering, Waseda University, Tokyo 160, Japan.

L.O.Chua is with the Department of Electrical Engineering and Computer Science, University of California, Berkeley, CA 94720

I. Introduction

This note reports an extremely simple cloning template for CNN (Cellular Neural Network) capable of detecting the "shadow" cast by a 2-dimensional image. The operation of this new template is best illustrated by the following simple example. Consider the 64×64 bipolar(±1) image shown in Fig.1 (a handwritten Japanese character). Applying this input to an extremely simple CNN to be described below one obtains Fig.2, which is the "shadow" of Fig.1 when the "object" is illuminated by a "light source" coming from the right. This template is motivated by our effort in improving the recognition rates of handwritten characters which will be briefly explained below.

II. The Shadow Detector

Proposition

Consider the CNN[1]-[4] defined by

$$C\frac{dVx_{ij}}{dt} = -\frac{1}{Rx}Vx_{ij} + A * Vy_{ij} + B * Vu_{ij} + I \qquad (1)$$

$$Vy_{ij} = \frac{1}{2}(|Vx_{ij} + 1| - |Vx_{ij} - 1|) \equiv f(Vx_{ij}) \qquad 1 \le i \le M,\ 1 \le j \le N$$

where * denotes the two dimensional "convolution operator"[1]-[4]. Let $U=\{u_{ij}\} \in \mathbf{R}^{M\times N}$ be a given bipolar 2-d image and let

$$A = \boxed{0 \mid 2 \mid 2} \qquad B = \boxed{0 \mid 2 \mid 0} \qquad ,I = 0$$

$$Vxij(0) = +1, \qquad Vuij = \begin{cases} +1 & \text{if } u_{ij} = +1 \\ -1 & \text{if } u_{ij} = -1 \end{cases} \qquad (2)$$

Then, for all pixels(i,j),

(i) $Vx_{ij}(t)$ converges to a stable equilibrium,and

(ii) $Vxij(\infty) = 1$ for all pixels falling within the shadow of U.

Proof Without loss of generality assume Rx=1,C=1 in (1). In view of the row structure of the templates defined in (2), it suffices for us to prove the result for the *1-dimensional* case. Then (1) together with (2) can be described by

$$\frac{dVx_i}{dt} = -Vx_i + 2\,Vy_i + 2\,Vy_{i+1} + 2Vu_i \qquad (3)$$

where

$$Vy_i = \frac{1}{2}\{|Vx_i + 1| - |Vx_i - 1|\} \equiv f(Vx_i)$$

Letting $g(Vx_i;Vu_i) = -Vx_i + 2Vy_i + 2Vu_i$, one can recast (3) as

$$\frac{dVx_i}{dt} = g(Vx_i;Vu_i) + 2f(Vx_{i+1}) \qquad (4)$$

Since $Vu_{ij} = 1$ or -1, the function $g(Vx_i;Vu_i)$ can be plotted as two piecewise-linear functions of a single variable Vx_i, parametrized by $Vu_{ij} = 1$ or -1, as shown in Fig.3.

Consider first the right most pixel ($i = N$). Since $f(Vx_{N+1}) = 0$, by default, (4) simplifies to

$$\frac{dVx_N}{dt} = g(Vx_N;Vu_N)$$

The following trajectory motions follow directly from the ***dynamic route***[5] indicated in Fig.3:
(i) if $Vu_N = +1$, then $(Vx_N(0), \dot{Vx}_N(0)) =$ **a** where **a** is indicated in Fig.3, and $Vx_N(t)$ increases monotonically from 1 to 4, independent of the state of the other pixels. We will denote this motion compactly as follows:

$Vx_N(t) = +1 \uparrow +4$ monotonically as $t \to \infty$. (5)

It is also clear that

(ii) if $Vu_N = -1$, then $(Vx_N(0), \dot{Vx}_N(0)) =$ **b** and

$Vx_N(t) = +1 \downarrow -4$ monotonically as $t \to \infty$ (6)

where $\downarrow$ denotes "decreases monotonically".

Therefore

(i) if $Vu_N = +1$, then

$f(Vx_N(t)) \equiv +1$ for all $t \geq 0$,and (7)

(ii) if $Vu_N = -1$, then

$f(Vx_N(t)) = +1 \downarrow -1$ monotonically as $t \to \infty$ (8)

Next consider $i = N - 1$:

$$\frac{dVx_{N-1}}{dt} = g(Vx_{N-1};Vu_{N-1}) + 2f(Vx_N) \qquad (9)$$

Case 1 $\quad Vu_{N-1} = +1$

Since $(Vx_{N-1}(0), \dot{Vx}_{N-1}(0)) =$ **c**, (see Fig.4), it follows from (7) and (8) and the corresponding dynamic route that $(Vx_{N-1}(t), \dot{Vx}_{N-1}(t))$ is trapped within and on the boundary of the shaded region shown in Fig.4. This implies that

$$f(Vx_{N-1}(t)) \equiv +1 \qquad \text{for all } t \geq 0 \tag{10}$$

Since $Vx_{N-1}(t)$ can stop only at a point where $\dot{Vx}_{N-1}(t)=0$, it follows that $Vx_{N-1}(t)$ converges to a point on the line segment[2,6].

Case 2 $\quad Vu_{N-1} = -1$

Following a similar analysis as in Case1, it can be easily shown that $(Vx_{N-1}(t),\dot{Vx}_{N-1}(t))$ is trapped within a band bounded by the two piecewise-linear curves shown in Fig.5. First note that $(Vx_{N-1}(0),\dot{Vx}_{N-1}(0)) = \mathbf{d}$.

It follows from (7) that if $Vu_N = +1$, then

$$Vx_{N-1}(t) = +1 \uparrow +2 \text{ monotonically as } t \to \infty$$

,and hence

$$f(Vx_{N-1}(t)) \equiv +1 \qquad \text{for all } t \geq 0. \tag{11}$$

Now observe that given each value $k=2f(Vx_N)$, the function

$$g(Vx_{N-1};-1)+k$$

defines a piecewise-linear curve lying within the band given in Fig.5.

It follows from (8) that if Vu_N=-1, then $2f(Vx_N(t))$ decreases *monotonically* from +2 to -2 so that $(Vx_{N-1}(t),\dot{Vx}_{N-1}(t))$ *cannot* "move up" the family of piecewise-linear curves in Fig.5 (since the upper most curve can only move downwards), and have

$$Vx_{N-1}(t) \quad = +1 \downarrow -6 \tag{12}$$

Therefore, $Vx_{N-1}(t)$ first increases for a while, and then decreases monotonically. This implies that

$$f(Vx_{N-1}(t)) = +1 \downarrow -1 \text{ as } t \to \infty \tag{13}$$

Finally, consider a *general* pixel i described by (4). It is easy to show that $f(Vx_{i+1}(t))$ is a monotonic function of t even though $Vx_{i+1}(t)$ may not be.(see **Remark1** below) Using an argument similar to the case i = N - 1, one can show that

$$\boxed{f(V_i(t)) \text{ converges to } \begin{cases} +1 \text{ if } Vu_i = +1 \textit{ or } Vu_{i+1} = +1 \\ -1 \text{ if } Vu_i = -1 \textit{ and } Vu_{i+1} = -1 \end{cases}} \tag{14}$$

Remark1 Observe that the motion of $Vx_{N-1}(t)$ in (12) is *not* a monotonic function of t, whereas the function $f(V_i(t))$ in (13) is monotonic because

$$f(Vx_{N-1}(t)) \equiv 1$$

before $Vx_N(t)$ starts decreasing.

Remark2 It is extremely important to note that although each pixel receives the information only from its ***immediate neighborhood***, on the same row, the dynamics of the entire array is ***global*** in nature. In other words, each pixel ***cannot*** determine whether its output should be +1 or -1 by looking at ***only the input values*** of its immediate neighborhood. Shadow, naturally, is a global property. It cannot be overemphasized, therefore, the ***dynamics*** (3) plays a *crucial* role in processing a given image (initial condition). This is true also for the templates given in [2]-[4]. The ***hole-filler*** template[3] is particularly dramatic in this respect.

III. Motivation

Our motivation for introducing the "shadow" template comes from our continuing quest for a more efficient CNN character recognition system[2]. When the shadow detector described above is used in addition to the ***Connected Component Detector***(CCD)[2], the recognition rate of ***handwritten characters*** (numerals, alphabets, symbols, Japanese characters) increases significantly. This means that the output of the shadow detector contains valuable ***new*** feature, not revealed by the output from the CCD alone. Note, however, the CNN should not be directly used as inputs to a classifier (e.g. Back Prop. Paradigme)[2], because it has too many bits. To overcome this, we could use the "shadow" CNN as a preprocessor by feeding its output (e.g. the image in Fig.2) into a connected component detector[2] so that the relevant features are extracted (e.g. the shadow features of Fig.2 is shown in Fig.6). Since the features extracted from Fig.2 are different from those extracted when the image in Fig.1 is fed directly to a bank of connected component detectors, as described in [2], it is clear that the augmentation of a shadow CNN as a preprocessor can improve the recognition rate dramatically.

References

1. L.O.Chua and L.Yang,"Clellular Neural Networks:Theory",IEEE Trans.Circuits and Systems, vol CAS-32,Oct 1988, pp1257-1290.
2. T.Matsumoto,L.O.Chua, and H.Suzuki,"CNN Cloning Template:Connected Component Detector",IEEE Trans. CAS,in press
3. T.Matsumoto,L.O.Chua, and R.Furukawa,"CNN Cloning Template:Hole-Filler",IEEE Trans.CAS,in press
4. T.Matsumoto,L.O.Chua, and T.Yokohama,"Image Thinning with a Cellular Neural Network",IEEE Trans.CAS,in press
5. L.O.Chua, C.A.Desoer and E.S.Kuh, Linear and Nonlinear Circuits,McGraw-Hill, New York, 1988

Figure Captions

Fig.1 A typical handwritten Japanese character.

Fig.2 The output image from the "shadow" CNN when the imagefrom Fig.1 is applied as its inputs. This image can be interpreted as the shadow which results when a horrizontal light beam is applied from the right of the character.

Fig.3 When plotted as a function of Vx_i, the upper curve is represented by $g(Vx_i;+1)$ while the lower curve is $g(Vx_i;-1)$. The dynamic route is depicted by the bold segments.

Fig.4 At all times, the trajectories are trapped within the shaded region.

Fig.5 The dynamic route for an arbitrary pixel.

Fig.6 The features extracted from the CCD when the shadow image in Fig.2 is applied as its input.

Fig.1

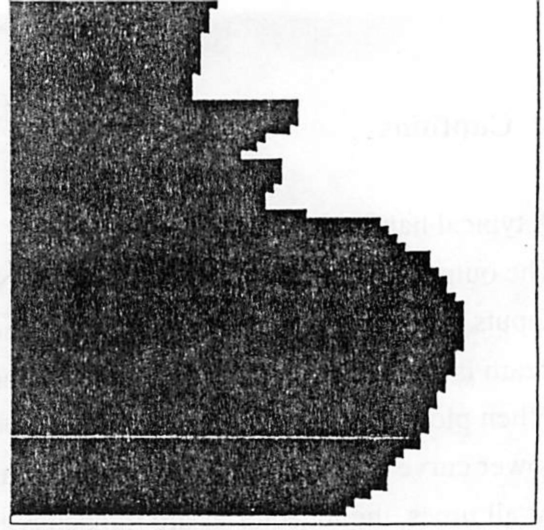

Fig.2

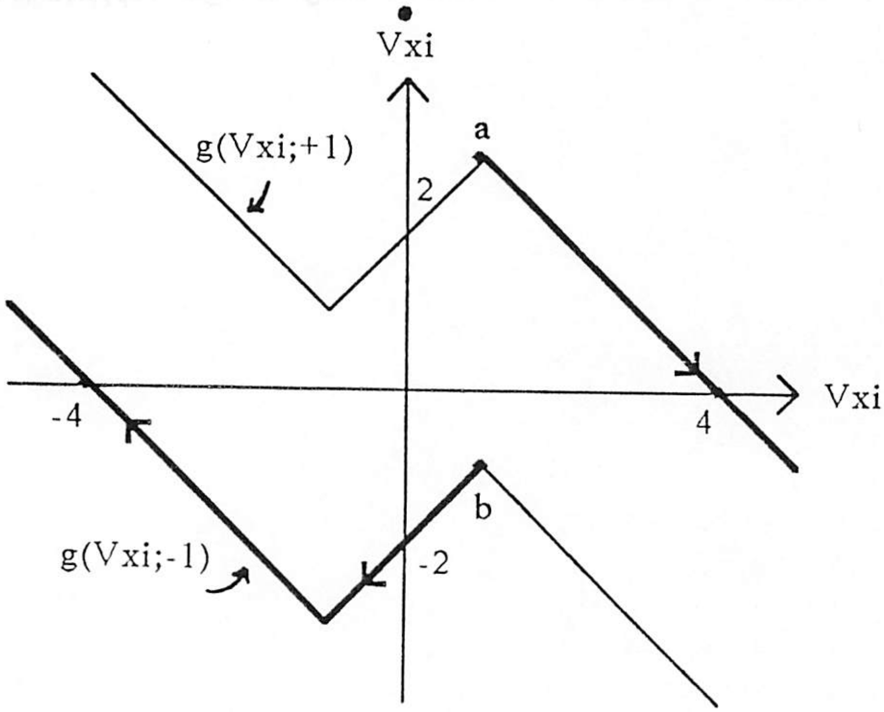

Fig.3

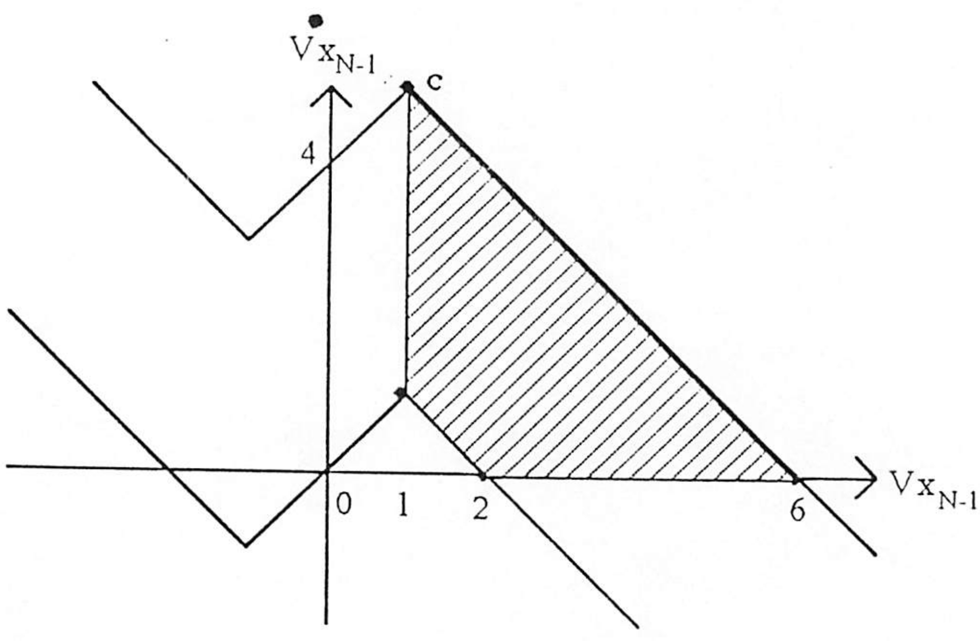

Fig.4

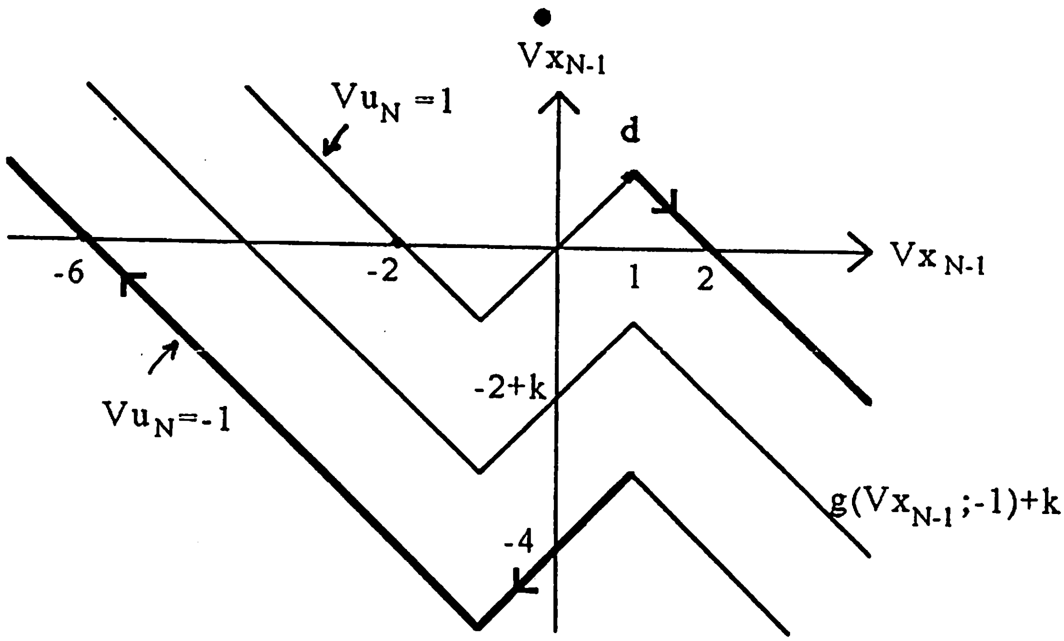

Fig.5

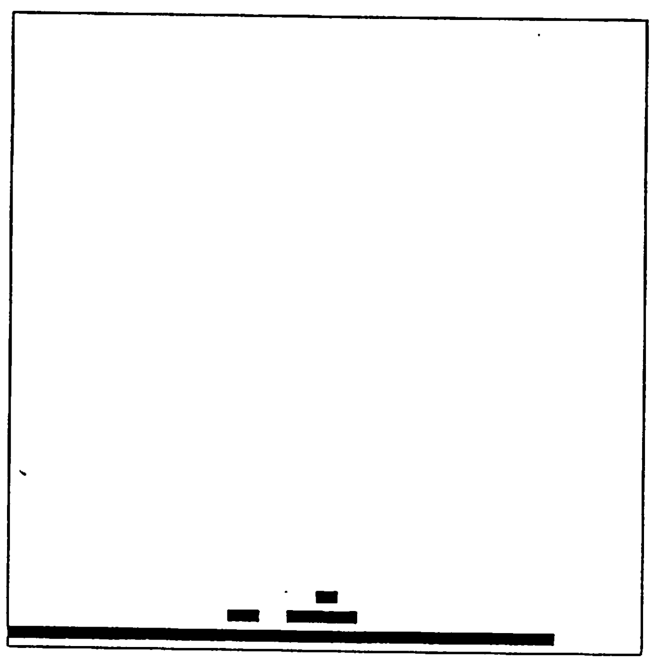

Fig.6